Kinetic and Mechanistic Analysis of a Reversible CO_2/HCO_2^- Electrocatalyst

*Drew W. Cunningham and Jenny Y. Yang**

Department of Chemistry, University of California, Irvine, USA, 92617

Table of Contents

Experimental 2
General considerations 2
Cyclic voltammetry 2
Synthesis of guanidinium•BPh_4 3
Solution preparation for proton transfer rate constant 3
Solution preparation for electron transfer rate constant 4
CO_2 insertion rates by NMR 4
CO_2 insertion rates by UV–Vis 5
Electron Transfer Rate Constant 5
Calculations 5
Figure S1. (a) Variable scan-rate CVs for (**1**) 7
Figure S2. Trumpet plot for determing k_{ET} for $[Pt(depe)_2]^{2+}$ 7
Protonation of $[Pt(depe)_2]$ to Generate $[HPt(depe)_2]^+$ 8
Figure S3. CVs of **1**, **1** with acid, and **3** 8
Figure S4. CVs and plot for $k_{obs,H+}$ determination 9
Figure S5. CVs and plot for $k_{obs,H+}$ determination: 9
Figure S6. $k_{obs,H+}$ for protonation of $Pt(depe)_2$ 10
Reaction of $Pt(depe)_2$ (**2**) with CO_2 10
Figure S7. CVs of $[Pt(depe)_2](PF_6)_2$ (**1**) (1.0 mM) with and without CO_2 10
Figure S8. Determination of k_{obs} for CO_2 binding. 11
Figure S9. Determination of k_{obs} for CO_2 binding using Savéant method 12
Reaction of $[HPt(depe)_2]^+$ (3) with CO_2. 12
Figure S10. Absorbance data and time traces for reaction of $[HPt(depe)_2]^+$ (**3**) with CO_2 and added $LiNTf_2$ 14
Figure S11. CVs of $[Pt(depe)_2][PF_6]_2$ in the presence of $LiNTf_2$ 15

Figure S12. CVs of $[Pt(depe)_2][PF_6]_2$ in the presence of guanidinium 15

Experimental

General considerations. All manipulations were carried out under a dinitrogen atmosphere in dried glassware unless otherwise noted. All chemicals were used as received from commercial sources unless otherwise noted. All non-deuterated solvents were degassed by sparging with argon and then dried by passage through an alumina column under argon pressure on a Solvent Drying System (JC Meyer Solvent Systems) and stored over activated molecular sieves. Deuterated solvents were degassed by freeze-pump-thaw methods then dried over activated molecular sieves. $[Pt(depe)_2][PF_6]_2$,[1] $[HPt(depe)_2][PF_6]$,[1] and $CH_2(TBD)_2$[2], and $CH_2(TBD)_2{\bullet}HPF_6$[2] were synthesized according to previously reported procedures.

Errors are reported to one standard deviation and are represented in parentheses, which indicate the error of the digits prior. For example, k_{obs} = 74(11) 1/s is equivalent to k_{obs} = 74 ± 11 1/s.

Guanidinium tetraphenylborate. To a solution of guanidinium nitrate (211 mg, 1.72 mmol) in water (30 mL) was added sodium tetraphenylborate (590 mg, 1.72 mmol) dissolved in water (30 mL). This resulted in the formation of a white precipitate, which was isolated after stirring for ca. 10 min by suction filtration, washing with water, and drying in vacuo. ^{1}H NMR (CD_3CN, 600 MHz): δ (ppm) = 5.91 (s br, 6H, NH_2), 6.84 (t, 4H), 6.99 (t, 8H), 7.27 (t, 8H).

Cyclic voltammetry. CVs were performed on a Pine Wavedriver 10 potentiostat with AfterMath software, using a 1 mm diameter glassy carbon disc working electrode and glassy carbon rod counter electrode. A Ag/Ag^+ pseudo-reference electrode containing a silver wire submerged in 0.2 M [*n*-Bu_4N][PF_6] separated from the bulk solution by a Vycor tip was used in addition to an internal ferrocene reference. It is important to note, that for kinetics experiments

(especially at high scan rates) that the IR drop was compensated for and that ferrocene was added as an internal reference for experiments that required precise determination of peak potentials (for rate determination) and each CV was carefully referenced individually.

Solution preparation for proton transfer rate constant. A stock solution of $[Pt(depe)_2][PF_6]_2$ was prepared by recording the mass of $[Pt(depe)_2][PF_6]_2$ (23.7 mg, 0.0264 mmol) directly in a 25.00 mL volumetric flask and dissolving with $CH_3CN/TBAPF_6$ (0.2 M). The working solution for CV measurements was then prepared by weighing $CH_2(TBD)_2{\bullet}H^+$ (21.0 mg, 0.481 mmol) directly into a 5.00 mL volumetric flask and dissolving with the $[Pt(depe)_2][PF_6]_2$ stock solution that was previously prepared. The resulting solution was 1.06 mM in $[Pt(depe)_2](PF_6)_2$ (**1**) and 9.62 mM in $CH_2(TBD)_2{\bullet}H^+$. This was repeated for different concentrations of $CH_2(TBD)_2{\bullet}H^+$ by weighing out differing amounts and dissolving in the same $[Pt(depe)_2](PF_6)_2$ (**1**) stock solution. CVs were then recorded with an aliquot of this solution. The data points are an average of 3 data points for each scan rate and errors are reported to one standard deviation.

Solution preparation for electron transfer rate constant. A 153 mM of $[Pt(depe)_2][PF_6]$ stock solution in CH_3CN (16.4 μL) was added to a 5.00 mL volumetric flask along with a 103 mM ferrocene stock solution in CH_3CN (21.3 μL) and diluted with $CH_3CN/TBAPF_6$ (0.2 M). The resulting solution was 0.501 mM in $[HPt(depe)_2]^+$ (**3**) and 0.499 mM in ferrocene. CVs were then recorded with an aliquot of this solution. The data points are an average of 3 data points for each scan rate and errors are reported to one standard deviation.

Reactivity of CO_2 with $[HPt(depe)_2][PF_6]$ by NMR. $[HPt(depe)_2][PF_6]$ (82.5 mg, 0.109 mmol) was weighed directly into a 5.00 mL volumetric flask. A small amount of CD_3CN (ca. 2 mL) was added to dissolve the platinum. C_6H_6 (9.00 μL) was added as an internal standard and

the remaining CD_3CN was added. The resulting solution was 21.9 mM in $[HPt(depe)_2]^+$ (**3**) and 26.4 mM in C_6H_6 and stored in the glovebox freezer at –35 ºC in between experiments. A 0.60 mL aliquot was put into a J-Young tube and an NMR spectra were acquired before the addition of CO_2. CO_2 was added by first pseudo-freeze-pump-thawing the J-Young tube on a custom-made gas-addition manifold composed of Swagelok pieces. To do this, a J-Young tube is attached to the manifold and the manifold is evacuated under dynamic vacuum and then shut off to vacuum once the pressure is < 50 mTorr. The J-Young tube is then briefly turned to open the valve to the static vacuum above it and then immediately closed. Dynamic vacuum is then once again applied to the manifold and the pressure increase on the gauge is noted. This procedure is then repeated until the solution is fully degassed, as indicated by a lack of pressure increase when applying dynamic vacuum after a cycle (usually three times would suffice). Once degassed, and after evacuating the manifold, it is then charged with CO_2 (1.0 atm). Immediately after charging with CO_2, a timer is started and this corresponds to $t = 0$. The J-Young tube is then quickly brought to and inserted into the pre-equilibrated spectrometer probe. For low temperature experiments, the procedure is the same except that the J-Young is first equilibrated in a cooling bath (water/ice for 5 ºC measurements and 9:1 ethanol/ethylene glycol –13 ºC measurements) for several hours until the temperature comes to a constant reading. The NMR probe is set to the temperature of the cooling bath and allowed to equilibrate for at least 15 minutes. NMR spectra are acquired before gas addition. Gas is then added as described above and NMR spectra are acquired over time. After acquiring the necessary spectra, a CH_3OH standard is used to calibrate the actual probe temperature.[4]

Reactivity of CO_2 with $[HPt(depe)_2][PF_6]$ by UV–Vis. These experiments were conducted in an identical fashion to the rates for NMR described above, except they were in a

1.0 cm path length quartz cuvette that had been adapted for connecting to the gas-addition manifold and at lowered concentrations achieved by serial dilution with volumetric glassware. The wavelength monitored was the λ_{max} of **3**, which was 247 nm.

Electron Transfer Rate Constant

Calculations. The electron transfer rate constants were calculated using the Butler-Volmer method where the peak potential of the anodic, E_{pa}, and cathodic, E_{pc}, waves shift with increasing scan rate given by the relationship given in eqs 2.1 and 2.2:

$$E_{pc} = E° - \frac{0.78RT}{n\alpha F} + \frac{2.303RT}{n\alpha F}\log\left(k_s\sqrt{\frac{RT}{n\alpha F\nu D}}\right) \tag{2.10}$$

$$E_{pa} = E° + \frac{0.78RT}{n(1-\alpha)F} + \frac{2.303RT}{n(1-\alpha)F}\log\left(k_s\sqrt{\frac{RT}{n(1-\alpha)F\nu D}}\right) \tag{2.11}$$

Where E^o is the formal reduction potential, R is the ideal gas constant, T is the absolute temperature, n is the number of electrons transferred, F is Faraday's constant, α is the so-called charge transfer coefficient, ν is the scan rate, and D is the diffusion constant. Electron transfer parameters (α and k_s) are determined by plotting E_p against the log of the scan rate. α is first calculated from the slope of the linear fit and then k_s is calculated from the y-intercept of each plot and reported as an average of the two.

In order to calculate the electron transfer rate constant, the diffusion coefficient, D, must first be determined. This is calculated from the Randles-Sevchik equation,[5] which describes the linear relationship for peak current a function of the square root of the scan rate:

$$i_p = 0.4463nFAC\sqrt{\frac{nF\nu D}{RT}} \tag{2.12}$$

Where n, F, C, D, R, and T are the same as previously defined; A is the electrode surface area in units of cm^2 and C is the concentration in units of mol/cm^3.

The variable-scan-rate CVs for $[Pt(depe)_2](PF_6)_2$ (**1**) can be seen in Figure 2.1a. From this data, the peak currents for the cathodic and anodic waves were plotted as the square root of the scan rate (Figure 2.1b) and D was calculated from the slope of each line and found to be 6.28×10^{-6} and 4.71×10^{-6} cm^2/s for the reduction and oxidation events, respectively.

As the scan rate, v, is increased and begins to exceed the diffusion of the species to and from the electrode, the change in peak potential, or ΔE_p, becomes larger and displays a linear relationship with the $\log(v)$. The scan-rate dependent CVs for $[Pt(depe)_2](PF_6)_2$ (**1**) at higher scan rates can be seen in Figure 2.2a and their corresponding peak potentials are shown in Figure 2.2b. From the slope of the linear portion of the cathodic wave, the electron transfer symmetry coefficient, α, was determined to be 0.20.

The electron transfer rate constant, k_{ET}, was then calculated from the y-intercepts of both the cathodic and anodic waves and determined to be 0.028 and 0.11 cm/s and is typically reported as an average, thus k_{ET} = 0.069(80) cm/s. Using the same CVs, the electron transfer rate constant for ferrocene was determined to be 0.32 cm/s, which is in good agreement with the k_{ET} often reported in the literature of 0.25 cm/s.[6]

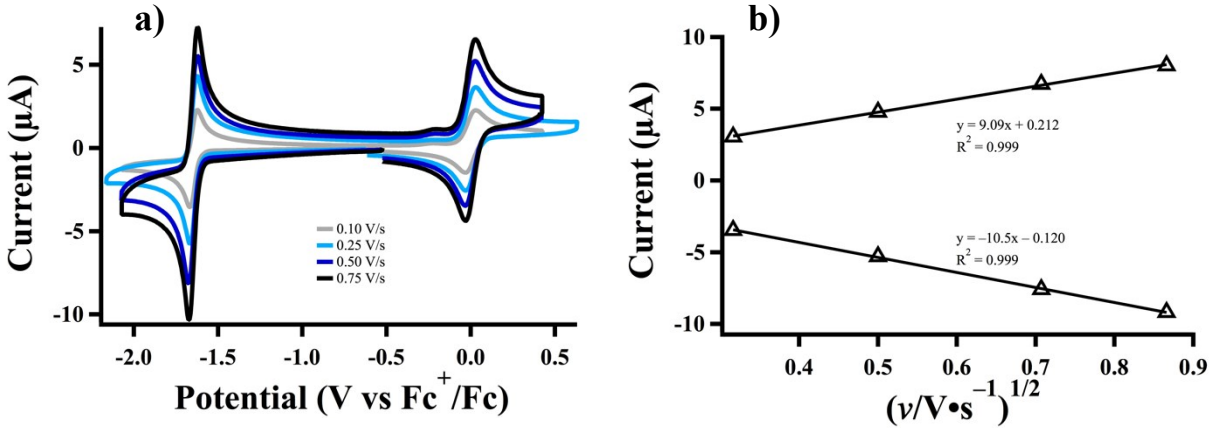

Figure S1. (a) Variable scan-rate CVs for $[Pt(depe)_2](PF_6)_2$ (1) (0.501 mM) in CH_3CN and (b) peak currents plotted as a function of the square root of scan rate for calculation of diffusion coefficient.

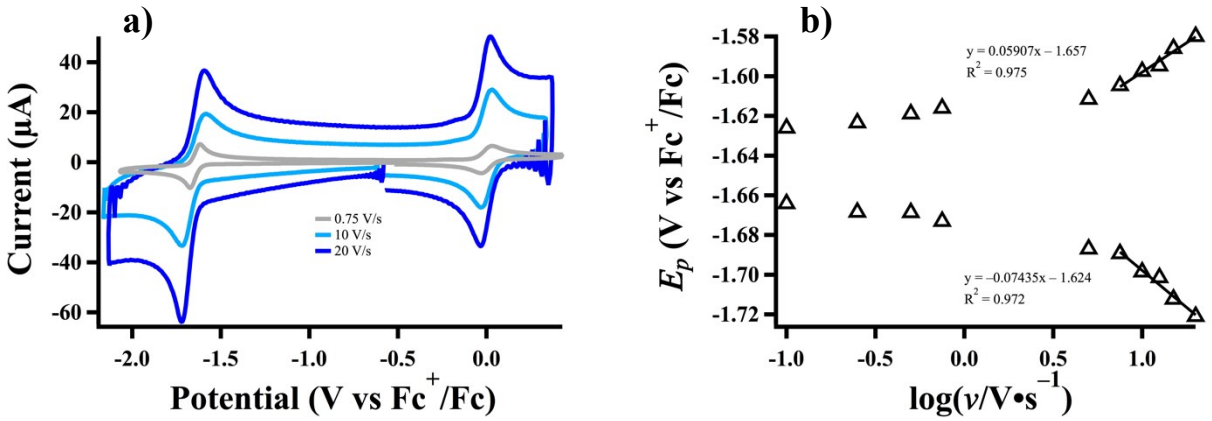

Figure S2. Trumpet plot. (a) Variable scan-rate CVs for $[Pt(depe)_2](PF_6)_2$ (**1**) (0.501 mM) in CH_3CN and (b) peak potentials plotted as a function of the logarithm of scan rate for calculation of electron transfer rate constant.

Protonation of $[Pt(depe)_2]$ to Generate $[HPt(depe)_2]^+$

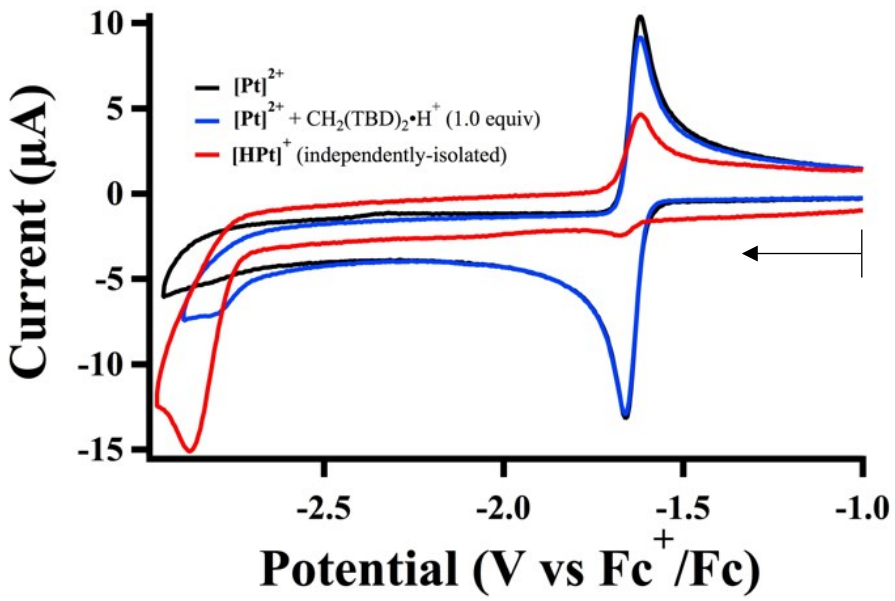

Figure S3. CVs of **1**, **1** with acid, and **3**. Scan rates are 0.250 V/s; the arrow represents the scanning direction and starting potential. In the red trace, the reductive feature at ca –1.6 V results from the formation of **1** due to trace amounts of water in the electrochemical setup.

For a chemical event that proceeds an electron-transfer event, or an EEC mechanism, the peak potentials shift cathodically relative to the formal potential with increasing scan rate. (eq 1).[7] All other constants are as previously defined. By plotting the change in peak potential as a function of the natural logarithm of the scan rate, the observed rate constant for protonation, $k_{obs,H+}$, was calculated from the y-intercept of the linear fit.

(eq 1) $$\frac{nF}{RT}\left(E_p - E^{\circ'}\right) = -0.780 + \frac{1}{2}\ln k_{obs,H+} + \frac{1}{2}\ln\frac{RT}{nF} - \frac{1}{2}\ln v$$

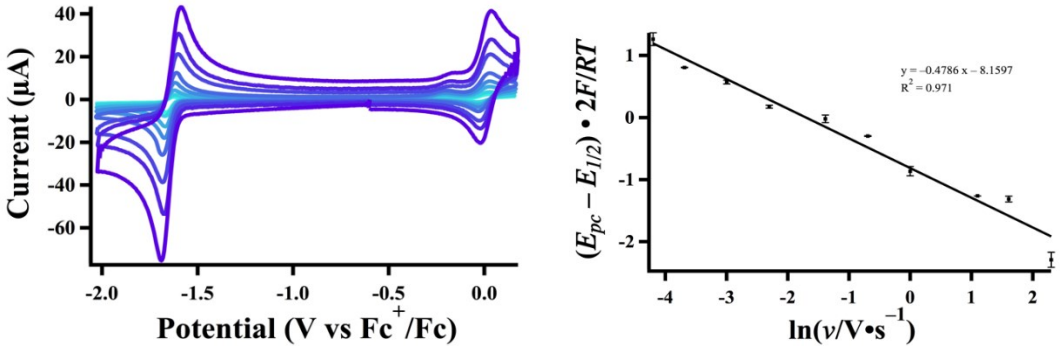

Figure S4. CVs and plot for $k_{obs,H+}$ determination: (a) Variable scan-rate CVs (0.05–10 V/s) of $[Pt(depe)_2](PF_6)_2$ (**1**) (1.06 mM) with $CH_2(TBD)_2•H^+$ (9.62 mM) and (b) linear plot for the change in cathodic peak potential for calculating $k_{obs,H+}$.

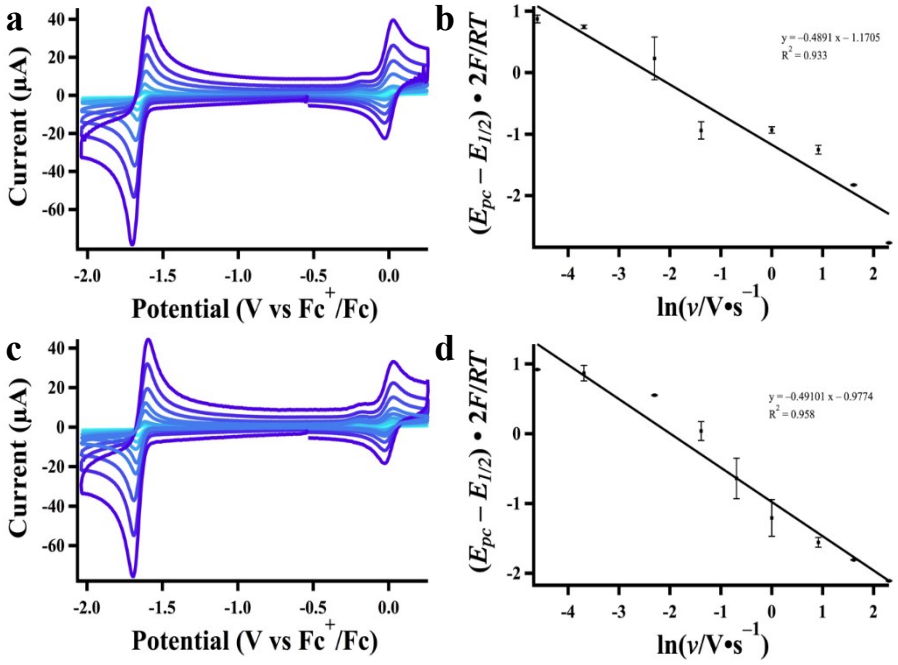

Figure S5. CVs and plot for $k_{obs,H+}$ determination: (a) Variable scan-rate CVs (0.025–10 V/s) of $[Pt(depe)_2](PF_6)_2$ (**1**) (1.06 mM) with $CH_2(TBD)_2•H^+$ (5.00 mM) and (b) linear plot for the change in cathodic peak potential for calculating $k_{obs,H+}$. (c) and (d) are the same experiment, but with 7.47 mM $CH_2(TBD)_2•H^+$.

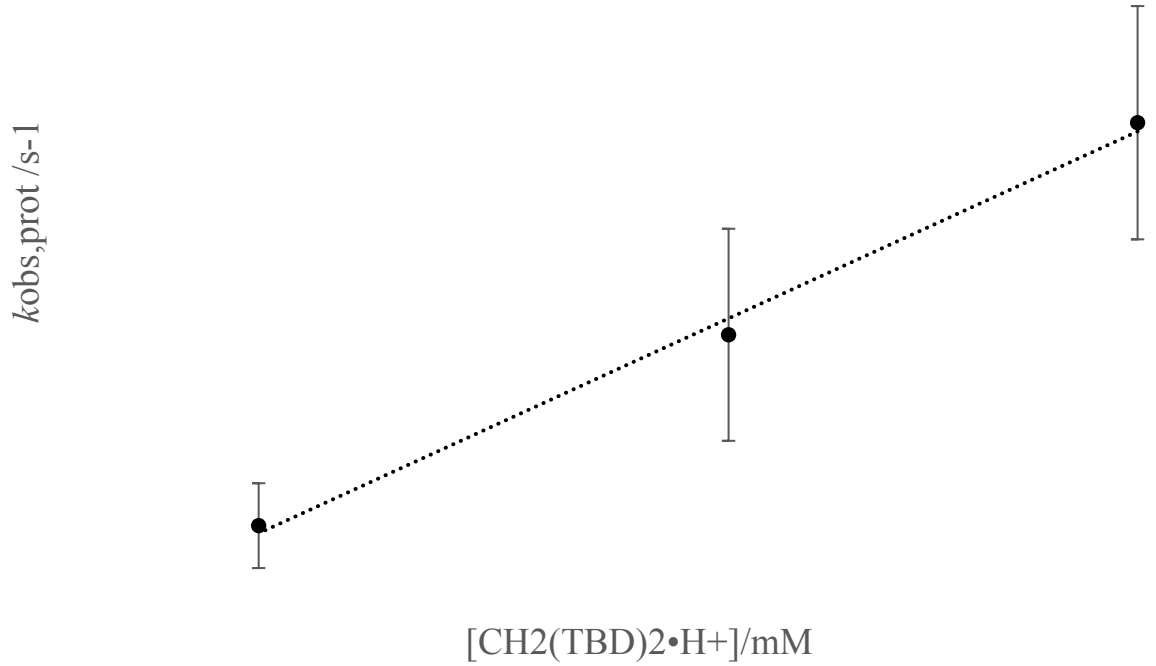

Figure S6. $k_{obs,H+}$ for protonation of $Pt(depe)_2$ (**2**) at various concentrations of $CH_2(TBD)_2•H^+$ to determine the 2nd order rate constant.

Reaction of $Pt(depe)_2$ (2) with CO_2

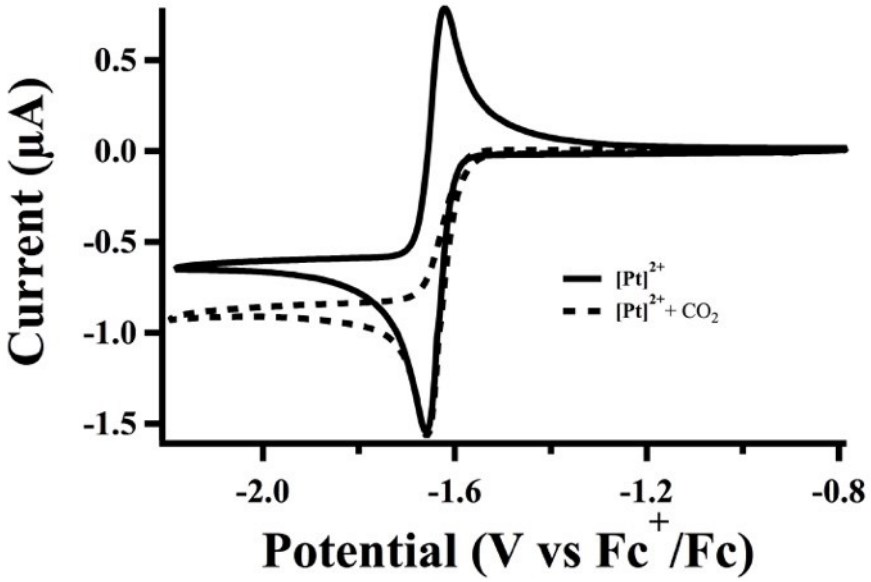

Figure S7. CVs of $[Pt(depe)_2](PF_6)_2$ (**1**) (1.0 mM) with and without CO_2 at a scan rate of 0.1 V/s.

The rate of CO_2 binding to $Pt(depe)_2$ (**2**) was then investigated to see how this rate compared to the rate of CO_2 insertion to $[HPt(depe)_2]^+$ (**3**). This was done by increasing the scan rate until the wave begins to have reversible character. In this method, described by DuBois, the peak ratio is proportional to the concentration of $Pt(depe)_2$ (**2**), and is plotted versus the time of the CV experiment to obtain an observed rate constant.[8] The plot of peak currents as a function of the scanning time can be seen in Figure S8. This plot is fit to a 3rd-order polynomial and from this the half-life was calculated to be 26 s, which corresponds to an observed rate constant, k_{obs}, of 0.023 s^{-1}.

To ensure more certainty in this number, the rate was also calculated another method described by Savéant (S9).[9] In this method, the peak current ratio is plotted against the natural logarithm of the scan rate. The plot should exhibit a sigmoidal curve and is fitted with a polynomial to determine the half-life. Using this method, k_{obs} was calculated to be 0.027 s^{-1}. These numbers are in good agreement with one another, and the observed rate constant for CO_2 binding was calculated as an average of the two to be 0.025(3) s^{-1}. The rate for CO_2 binding by $Pt(depe)_2$ (**2**) is much less than the rate for protonation of $Pt(depe)_2$ (**2**) (>750 s^{-1} under catalytic conditions), thus this kinetic bifurcation point would favor protonation of $Pt(depe)_2$ (**2**) over CO_2 binding.

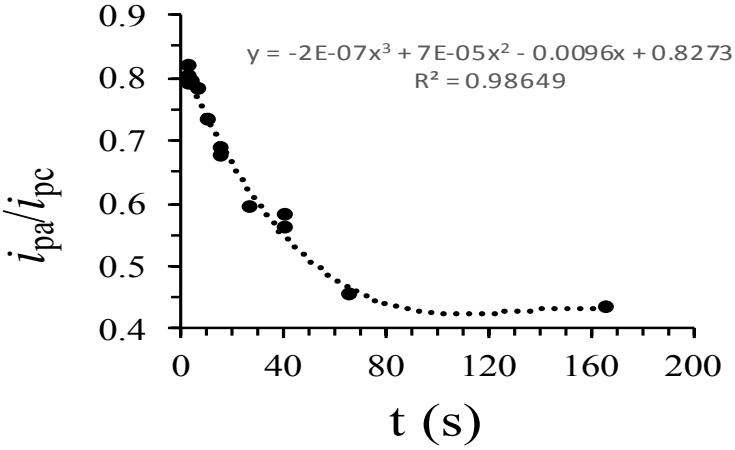

Figure S8. Determination of k_{obs} for CO_2 binding. Peak intensities from a series of scan-rate dependent CV experiments with $[Pt(depe)_2](PF_6)_2$ (**1**) (0.50 mM) and CO_2 (1 atm, 280 mM)

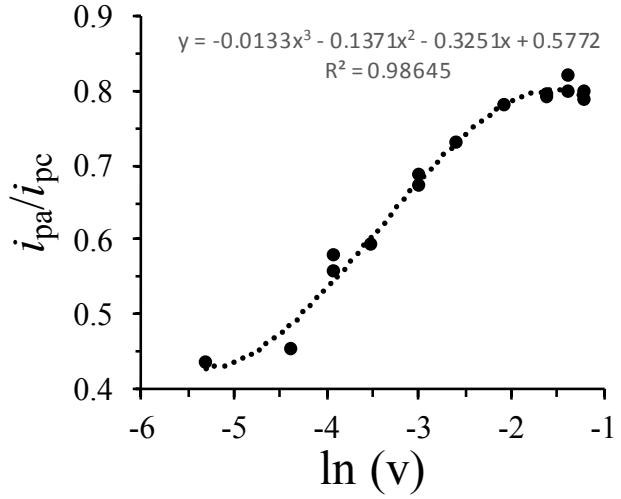

Figure S9. Determination of k_{obs} for CO_2 binding using Savéant method. Peak ratios plotted at different scan rates for the reaction of $[Pt(depe)_2](PF_6)_2$ (**1**) (1.0 mM) and CO_2 (1.0 atm, 280 mM).

Reaction of $[HPt(depe)_2]^+$ (3) with CO_2.

The rate constant, k_{obs}, was calculated by the method of initial rates by using the slope of the line containing the initial time points (t <15 min). The slope of the initial data points represents the rate equation:

$$-\frac{d[HPt^+]}{dt} = -(slope) = k[HPt^+][CO_2] \qquad \text{(eq1)}$$

Under the experimental conditions, it is assumed the concentration of CO_2 is 280 mM[10] and is therefore in >10-fold excess than $[HPt(depe)_2]^+$ (**3**) and the rate expression becomes:

$$-\frac{d[HPt^+]}{dt} = -(slope) = k_{obs}[HPt^+] \quad \text{(eq 2)}$$

At room temperature, 40% of the initial $[HPt(depe)_2]^+$ (**3**) was consumed after 100 min and the observed rate constant was calculated to be 2.8×10^{-4} s^{-1}.

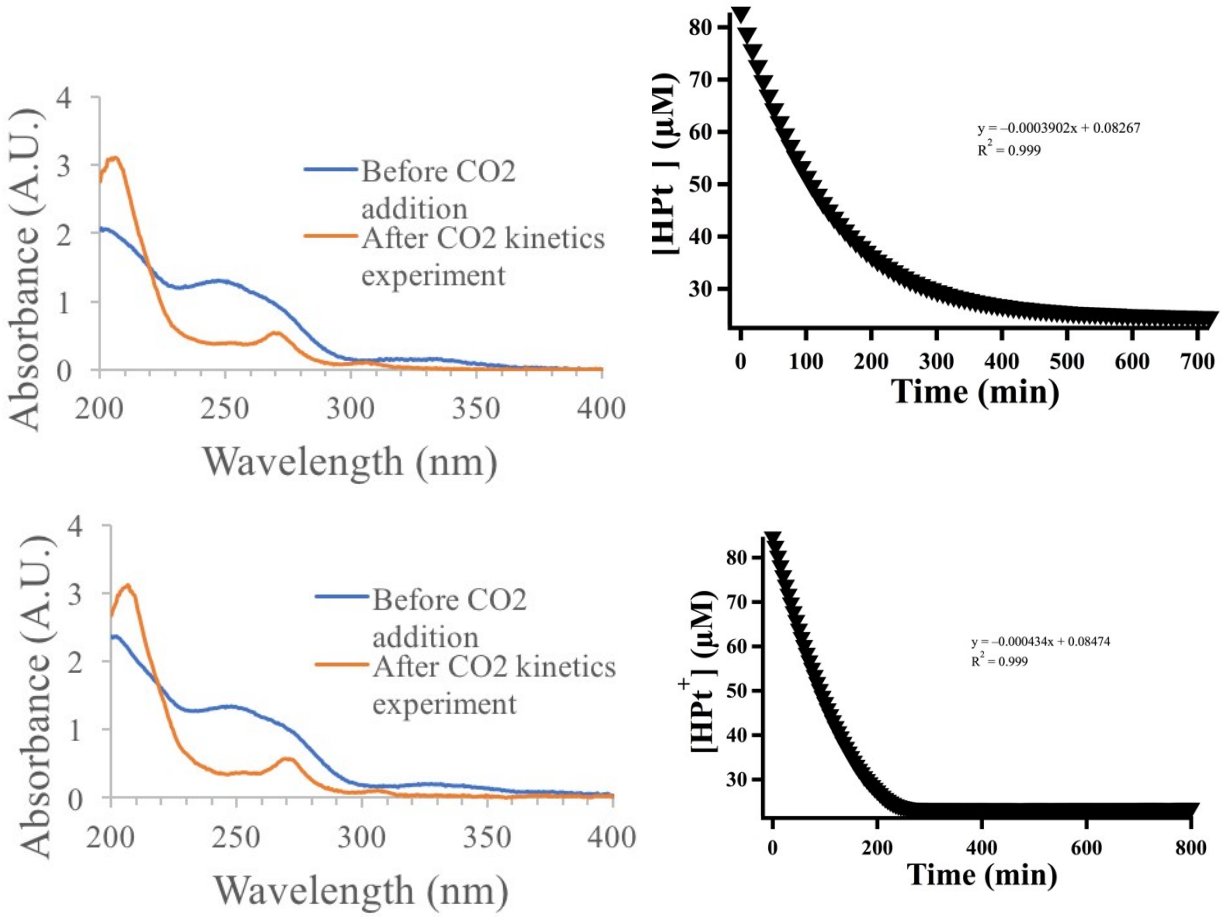

Figure S10. Absorbance spectra and time traces for the reaction of $[HPt(depe)_2]^+$ (0.100 mM) with CO_2 (1.0 atm) in the absence and presence of added $LiNTf_2$: (top) in the absence of any additives and (bottom) in the presence of added $LiNTf_2$ (10 mM). The time traces on the right were acquired at 247 nm and the linear fits were determined using the data for which $t < 20$ min.

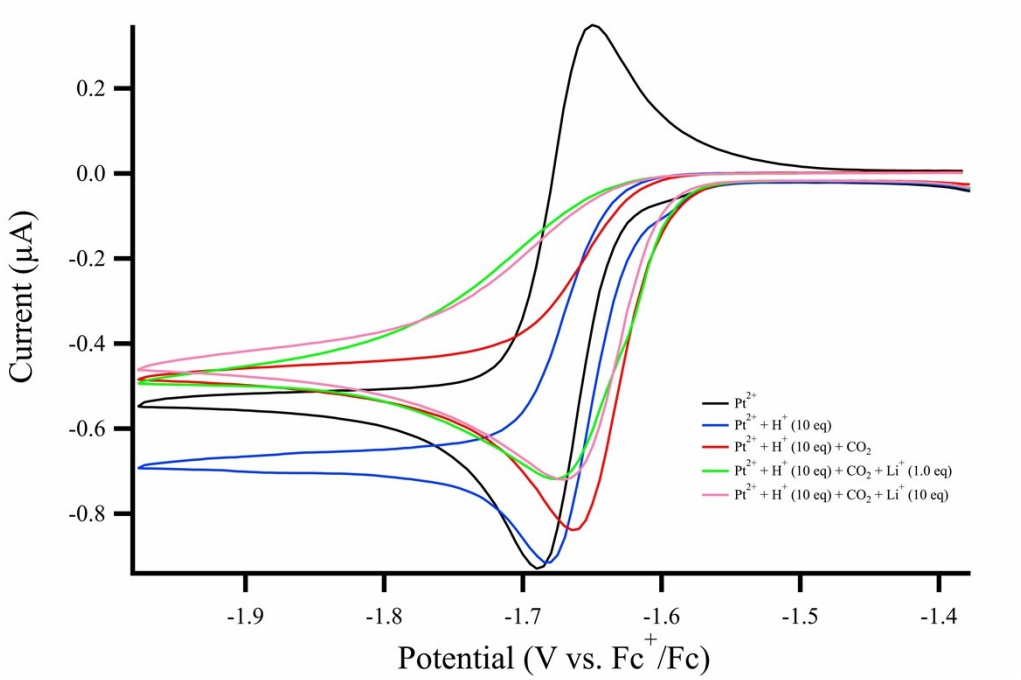

Figure S11. CVs of $[Pt(depe)_2][PF_6]_2$ (1.0 mM) with $CH_2(TBD)_2 \bullet H^+$ (H^+) and varying amounts if $LiNTf_2$ (Li^+) with a CO_2-saturated acetonitrile solution. Scan rate is 5 mV/s.

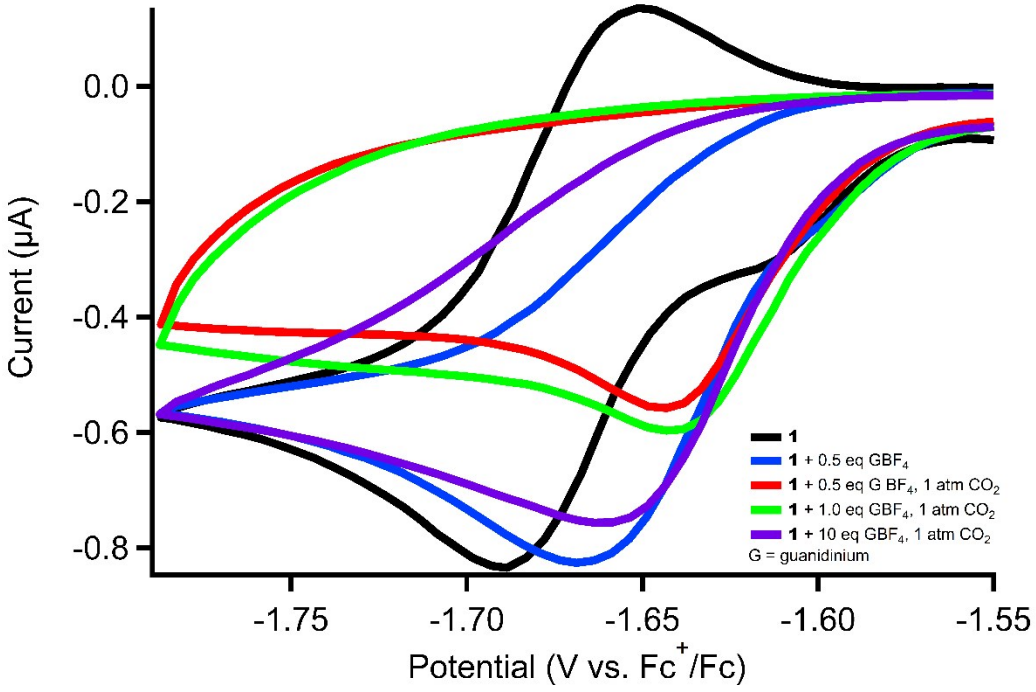

Figure S12. CVs of $[Pt(depe)_2][PF_6]_2$ (0.49 mM) with varying amounts of guanidinium tetraphenylborate in a CO_2-saturated acetonitrile solution. Scan rate is 5 mV/s.

References

1. Miedaner, A.; DuBois, D. L.; Curtis, C. J.; Haltiwanger, R. C., Generation of metal formyl complexes using nickel and platinum hydrides as reducing agents. *Organometallics* **1993,** *12* (2), 299-303.
2. Oakley, S. H.; Coles, M. P.; Hitchcock, P. B., Structural and Catalytic Properties of Bis(guanidine)copper(I) Halides. *Inorg. Chem.* **2003,** *42* (10), 3154-3156.
3. Coles, M. P.; Aragón-Sáez, P. J.; Oakley, S. H.; Hitchcock, P. B.; Davidson, M. G.; Maksić, Z. B.; Vianello, R.; Leito, I.; Kaljurand, I.; Apperley, D. C., Superbasicity of a Bis-guanidino Compound with a Flexible Linker: A Theoretical and Experimental Study. *J. Am. Chem. Soc.* **2009,** *131* (46), 16858-16868.
4. Vo, T.; Purohit, K.; Nguyen, C.; Biggs, B.; Mayoral, S.; Haan, J. L., Formate: an Energy Storage and Transport Bridge between Carbon Dioxide and a Formate Fuel Cell in a Single Device. *ChemSusChem* **2015,** *8* (22), 3853-3858.
5. Bard, A. J., *Electrochemical methods : fundamentals and applications / Allen J. Bard, Larry R. Faulkner*. Wiley: New York, 1980.
6. Mashkina, E.; Bond, A. M., Implementation of a Statistically Supported Heuristic Approach to Alternating Current Voltammetric Harmonic Component Analysis: Re-evaluation of the Macrodisk Glassy Carbon Electrode Kinetics for Oxidation of Ferrocene in Acetonitrile. *Anal. Chem.* **2011,** *83* (5), 1791-1799.
7. Saveánt, J. M., *Elements of Molecular and Biomolecular Electrochemistry: An Electrochemical Approach to Electron Transfer Chemistry*. Wiley: Hoboken, NJ, 2006.
8. Yang, J. Y.; Bullock, R. M.; Shaw, W. J.; Twamley, B.; Fraze, K.; DuBois, M. R.; DuBois, D. L., Mechanistic Insights into Catalytic H2 Oxidation by Ni Complexes Containing a Diphosphine Ligand with a Positioned Amine Base. *J. Am. Chem. Soc.* **2009,** *131* (16), 5935-5945.
9. Savéant, J. M., Investigation of Rates and Mechanisms of Reactions. In *Investigation of Rates and Mechanisms of Reactions* Wiley, Ed. 1986.
10. Fujita, E.; Szalda, D. J.; Creutz, C.; Sutin, N., Carbon dioxide activation: thermodynamics of carbon dioxide binding and the involvement of two cobalt centers in the reduction of carbon dioxide by a cobalt(I) macrocycle. *J. Am. Chem. Soc.* **1988,** *110* (14), 4870-4871.